



**INTERNATIONAL JOURNAL OF
PHARMACEUTICAL SCIENCES**
[ISSN: 0975-4725; CODEN(USA): IJPS00]
Journal Homepage: <https://www.ijpsjournal.com>



Research Article

Antimicrobial Characteristics Of Certain Polymeric Materials Containing Guanidine And Hydrazine Derivatives

L. Edwin Paul¹, M. Shanmugavel², P. Balashanmugam³, S. Thennarasu⁴, V. Jaisankar^{*5}

¹Department of Organic and Bioorganic Chemistry Lab, CSIR- Central Leather Research Institute (CLRI), Adyar, Chennai-600020, Tamil Nadu, India

²Department of Microbiology Lab, CSIR-Central Leather Research Institute (CLRI), Adyar, Chennai 600020, Tamil Nadu, India

³Avigenbiotech Pvt Ltd, Chrompet, Chennai-600044, Tamil Nadu, India

⁴Department of Organic and Bioorganic Chemistry Lab, CSIR- Central Leather Research Institute (CLRI), Adyar, Chennai-600020, Tamil Nadu, India

⁵PG and Research Department of Chemistry, Presidency College (Autonomous), Chennai 600 005, Tamil Nadu, India

ARTICLE INFO

Received: 28 July 2024

Accepted: 30 July 2024

Published: 31 July 2024

Keywords:

PMMA, antimicrobial, cell viability, apoptosis, cancer cell lines

DOI:

10.5281/zenodo.13140816

ABSTRACT

Polymeric materials are extensively utilized in a variety of biomedical applications due to their versatile physicochemical characteristic properties. In this study, we report that polymer-based amide-designed compounds with antibacterial and anticancer activities were employed to modify the antimicrobial characteristics of linear polymer functional moieties. New moderately hydrophobic linear polymer structures, including the guanidine and Hydrazine hydrate derivative with hydrazide linkage or amide bond linkage, have been constructed and investigated in conjunction with these developments. The method was useful in developing PMMA derivatives from guanidine hydrochloride and Hydrazine monohydrate as potential antibacterial agents. Chemically modified compounds were characterized FT-IR, NMR, GPC, TGA&DSC, DLS and FESEM analysis. Preliminary biological tests have shown that polymers have a high acceptance level of bactericidal activity to be employed as standalone high antimicrobial preparations or as effective additives in composite materials. These polymeric materials were characterized for optimal physicochemical properties of the products that have been studied. Likewise, the PMMA-modified compounds were also evaluated for cell viability against the A549 cancer cell line. The results indicated that PMMA-G and

***Corresponding Author:** V. Jaisankar

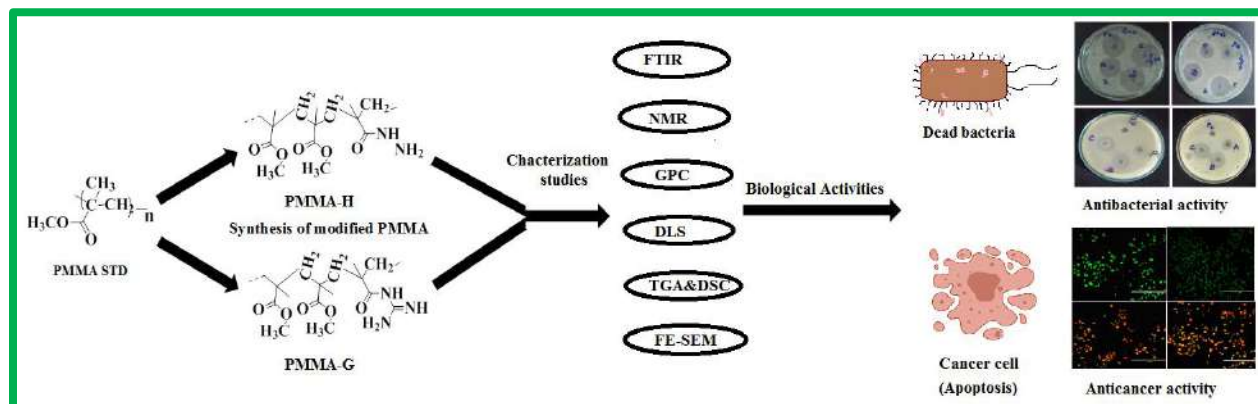
Address: PG and Research Department of Chemistry, Presidency College (Autonomous), Chennai 600 005, Tamil Nadu,

Email ✉: vjaisankar@gmail.com

Relevant conflicts of interest/financial disclosures: The authors declare that the research was conducted in the absence of any commercial or financial relationships that could be construed as a potential conflict of interest.



PMMA-H have higher anticancer activity in a short period of 24 hours while PMMA less anticancer activity. Furthermore, the AO/PI staining assay was used to test and fluorescence microscopy was used to confirm the apoptosis in cancer cell lines.



INTRODUCTION

In recent years, PMMA modified polymers are employed in various medical applications. The ester group of PMMA polymer converted to amide linkage in derivatization employed as a key structural motif in various biological activities like antibacterial and anticancer activities. PMMA modified with hydrazine monohydrate and guanidine hydrochloride¹ results in selective structural and biological characteristics. Modified PMMA polymers are expected to possess more biological effectiveness compared to conventional biomedical polymers. Biologically important modified PMMA derivative with amide and carbonyl group in chemical structure extensively used in medicine². The presence of hydrazide moiety in the polymerized compounds is considered in the medical field especially for anticancer activity. Antibacterial polymers served as a potential substitute for antibiotics. To bridge the gap between scientific research and actual or potential uses, the mechanism, benefits, and potential clinical applications of certain antibacterial polymers are synthesized and analysed in this work. Future designers and

developers of antibacterial medical devices are likely to find the information presented in this article to be a helpful tool.⁴⁻⁶ Lung cancer cell line were used to investigate anticancer activity for the modified PMMA compounds. Based on the survey, a comparative study of PMMA with modified PMMA-H and PMMA-G is explored.

2. Materials and methods

Poly (methyl methacrylate), Hydrazine monohydrate, and Guanidine hydrochloride were purchased from Sigma Aldrich. Base like Triethylamine is also purchased from Sigma Aldrich. Tetrahydrofuran (THF) and ethanol were purchased chemicals and solvents from Rankem and analytical reagents. DMSO-d₆ and CDCL₃ were used in the NMR spectral analysis purchased from Sigma Aldrich and Merck. All the substances were utilized without purification for synthesis and purification.

2.1 Synthesis of hydrazine modified PMMA

For the synthesis, 1g (10 mmol) of PMMA was taken in a 100 ml RB flask with an stirrer and 5 ml of THF was used to dissolve the starting material. After completely dissolving the polymer, 3ml (60mmol) hydrazine

*Corresponding Author: V. Jaisankar

Address: PG and Research Department of Chemistry, Presidency College (Autonomous), Chennai 600 005, Tamil Nadu,

Email ✉: vjaisankar@gmail.com

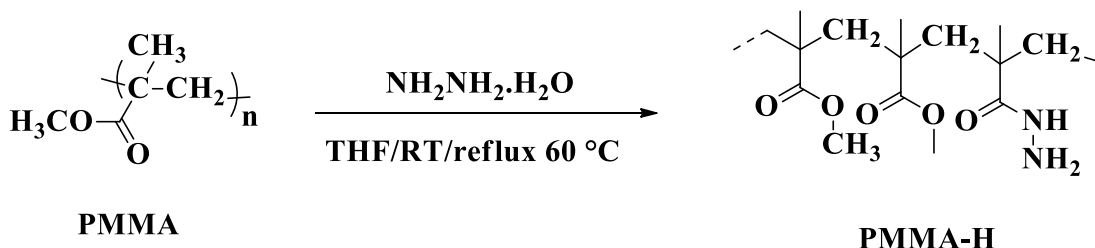
Relevant conflicts of interest/financial disclosures: The authors declare that the research was conducted in the absence of any commercial or financial relationships that could be construed as a potential conflict of interest.



monohydrate was added slowly to the reaction flask at the RT. After the reaction mixture was continuously stirred for 3 to 4 h at room temperature, and reflux condition was continued in an oil bath for 48h at 100 °C .

The obtained solid was filtered, washed several times with ethanol, dried under vacuum at 50 °C for 2h, and then kept in a hot air oven yielding an amorphous powder that was denoted as PMMA-H.

Scheme 1

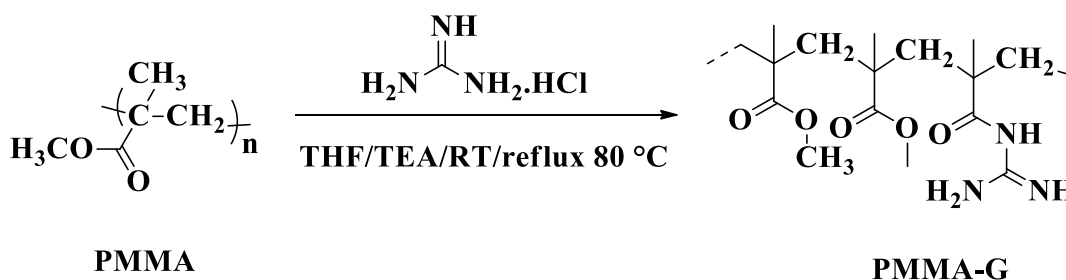


2.2 Synthesis of guanidine-modified PMMA.

PMMA was modified using guanidine in a 1:3 ratio, PMMA (3g), was dissolved in 5 ml THF. Guanidine hydrochloride (1g) was separately dissolved in 3 ml of DMF in a test tube and then transferred to the reaction flask. A magnetic stirrer was used to obtain a uniform solution. Triethylamine was added (1 ml) drop wise to the resulting solution under stirring. The

solution was refluxed in an oil bath at 120 °C for 72h. The product formation in the reaction mixture was product using FTIR. The the solid sediment in the RB flask was washed with a small amount of water (three times) to remove unreacted guanidine. The white precipitate was dried under air and then under vacuum to obtain an amorphous powder.

Scheme 2



2.3 Characterization.

FT-IR spectra were obtained on a Perkin Elmer spectrum Two UATR FT-IR spectrometer with KBr pellets containing modified linear polymer compound. The Spectra region is displayed with a resolution of 2 cm⁻¹, a scanning rate of 2 mm/s, and 20 scans in the frequency range of 4000–400 cm⁻¹. Especially the hydrazide group of modified polymer has identified and recorded the IR spectrum. 1H and 13C NMR spectra were

recorded on a BRUKER-DMX advance 400 MHz Spectrometer using CDCL₃ and Dmsod₆ as the solvent. The chemical shift values of the hydrazide or amide proton and carbon in the modified linear polymer molecule in the NMR spectrum serve as confirmation. The particle size distribution and Zeta potential of PMMA derivatives was observed by using Dynamic Light Scattering (Malvern Instruments Ltd, Malvern, UK). The evaluation of the thermal stability of PMMA

and modified linear polymers used Thermo gravimetric analysis (TGA) was conducted with, TA Instruments, SETARAM, THEMYS ONE+, KEP technologies, Switzerland, thermo gravimetric analyzer. Experiments were carried out on 1–6 mg samples heated in flowing under N₂ atmosphere at a heating rate of 5 °C/min. The temperature was employed as the measure for the amount of weight loss as a result of the volatile component's formation. The thermal analysis of PMMA and their modified derivatives were also carried out by using DSC 25, TA Instruments, and Waters Austria. The dynamic DSC run was recorded at a heating rate of (Ramp) 5°C/min under N₂ atmosphere. For each analysis about 2-3 mg of sample is used, and scans were recorded in the temperature range RT to 350°C. Gel permeation chromatography (GPC; Agilent technologies, model Agilent 1260, US) was used to determine the samples' average molecular weights and molecular weight distribution. Tetrahydrofuran was used as the elution solvent, and its flow rate was held constant at 0.5 mL/min. using RI detectors and wavelength absorbance 285 nm. The modified PMMA linear polymer compounds' microstructure image was captured using FE-SEM, an advanced technique (XFlash 410, Bruker Nano GmbH Berlin, Germany, Esprit 1.9).

2.4 Cell viability by MTT assay

The Lung cancer cell lines of A549 seeded in 96-well microplates (1 x 10⁶ cells/well) and incubated at 37°C for 72 h in 5% CO₂ incubator and allowed to grow 90% confluence. Then the medium was replaced and the cells were treated with PMMA sample and modified basis compounds PMMA-G and PMMA-Hat different concentration of such as 10, 20, 30, 40 and 50 µg/mL and incubated for 24 h. The cells were then washed with

phosphate-buffer saline (PBS, pH- 7.4) and 20 µL of (MTT) solution (5 mg/mL) was added to each well. The plates were then stand at 37°C in the dark for additional 4 hr. The formazan crystals were dissolved in 100 µL DMSO and the absorbance was read spectrometrically at 570 nm. The percentage of cell viability was expressed as formula.

$$\text{Cell viability (\%)} = \frac{\text{OD absorbance treated cell}}{\text{OD absorbance of control cell}} \times 100$$

The concentration that inhibited 50% of cell growth was referred as IC₅₀ value, which was used as a parameter for cytotoxicity study. The morphological changes of untreated (control) and treated cells were observed under the FLoid Cell Imaging Thermo Fisher – Invitrogen EVOS XL Model after 24 h and photographed.

2.5 Apoptosis assay of Modified PMMA compounds

Cell apoptosis was examined using Venugopal et al.'s (2017) protocol³⁶. Acridine orange/propidium iodide (AO/PI) staining served as a useful method for identifying cell growth. Using the minimum inhibitory strength of modified PMMA identified by the MTT assay, A549 cancer cells were seeded in 96-well plates and incubated for 24h. Following treatment, 5 µL of a fluorescent dye stain (acridine orange, 100 µg/mL) and 5 µL of propidium iodide (PI, 100 µg/mL) were added to the treated cells and washed with phosphate buffer saline. When AO dye binds to both viable and nonviable cells, it emits either red or green fluorescence; in contrast, PI emits only red fluorescence when it connects to nonviable cells. The morphological changes^{37,38} in the apoptotic nuclei

(intensely stained, fragmented nuclei and condensed chromatin) cells were observed
 Fluid Cell Imaging fluorescent microscope.

2.3.1 FTIR Spectrum

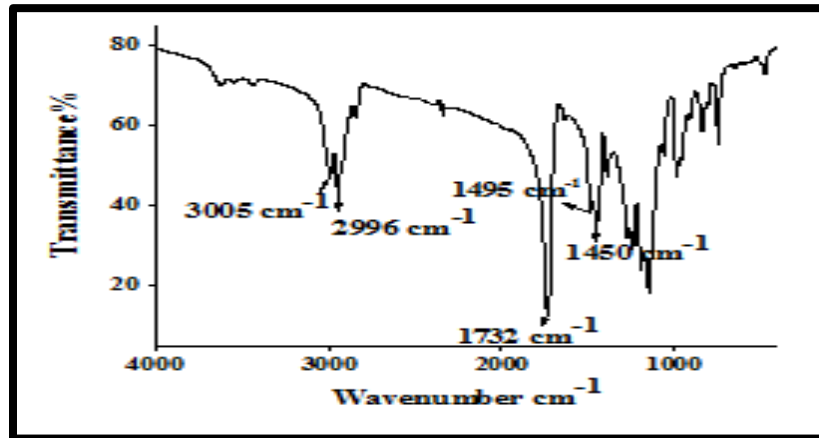


Fig1a:IR spectrum of PMMA

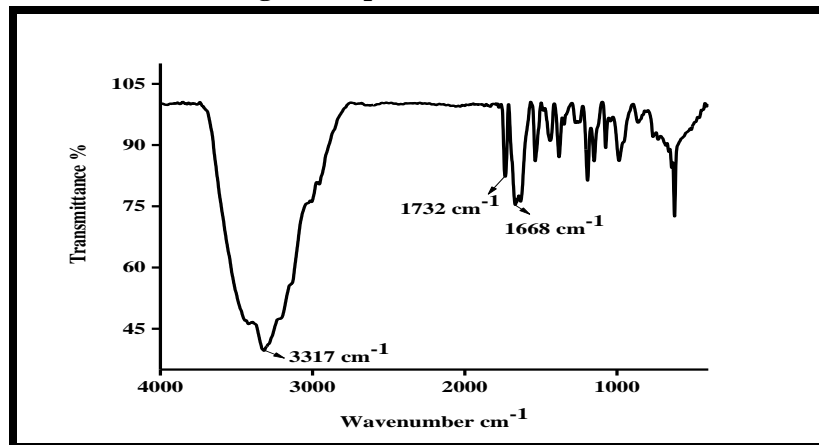


Fig 1b: IR spectrum of PMMA-G

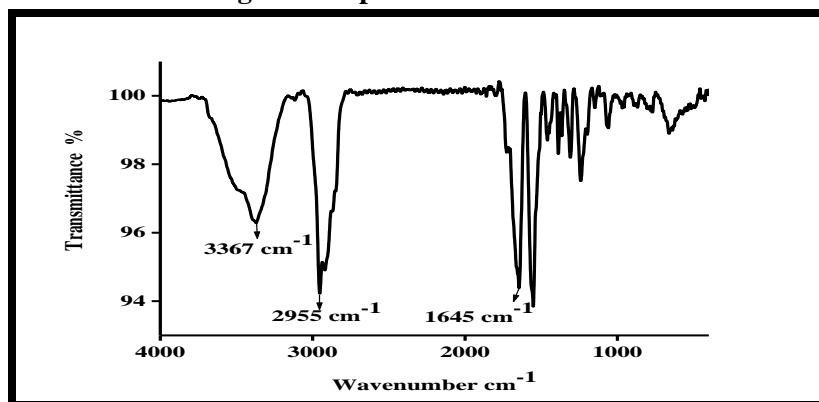


Fig 1c: IR spectrum of PMMA-H

PMMA (Figure 1a) modified with two basic compounds were characterized by FT-IR7. As shown clearly in Figure 1b and 1c, a strong absorption peak at 1668 cm⁻¹ and 1645 cm⁻¹

corresponding to stretching vibration of C=O bond is clearly observed for modified polymers, suggesting the formation hydrazide linkage or quinidine amide linkage. In the control spectrum

Fig 1a, the adsorption peak for C=O in the methyl ester bond is located at about 1732 cm⁻¹. The broad peaks centered at 3317 cm⁻¹ (Fig 1b) and 3367 cm⁻¹ (Fig 1c) suggest the multiple stretching

vibrations of CO-NH and CO-NH-NHR due to H-bonding. The absence of such a broad peak in the control polymer (Fig 1a) confirms the H-bonding in the modified polymers.

2.3.2 NMR Spectrum

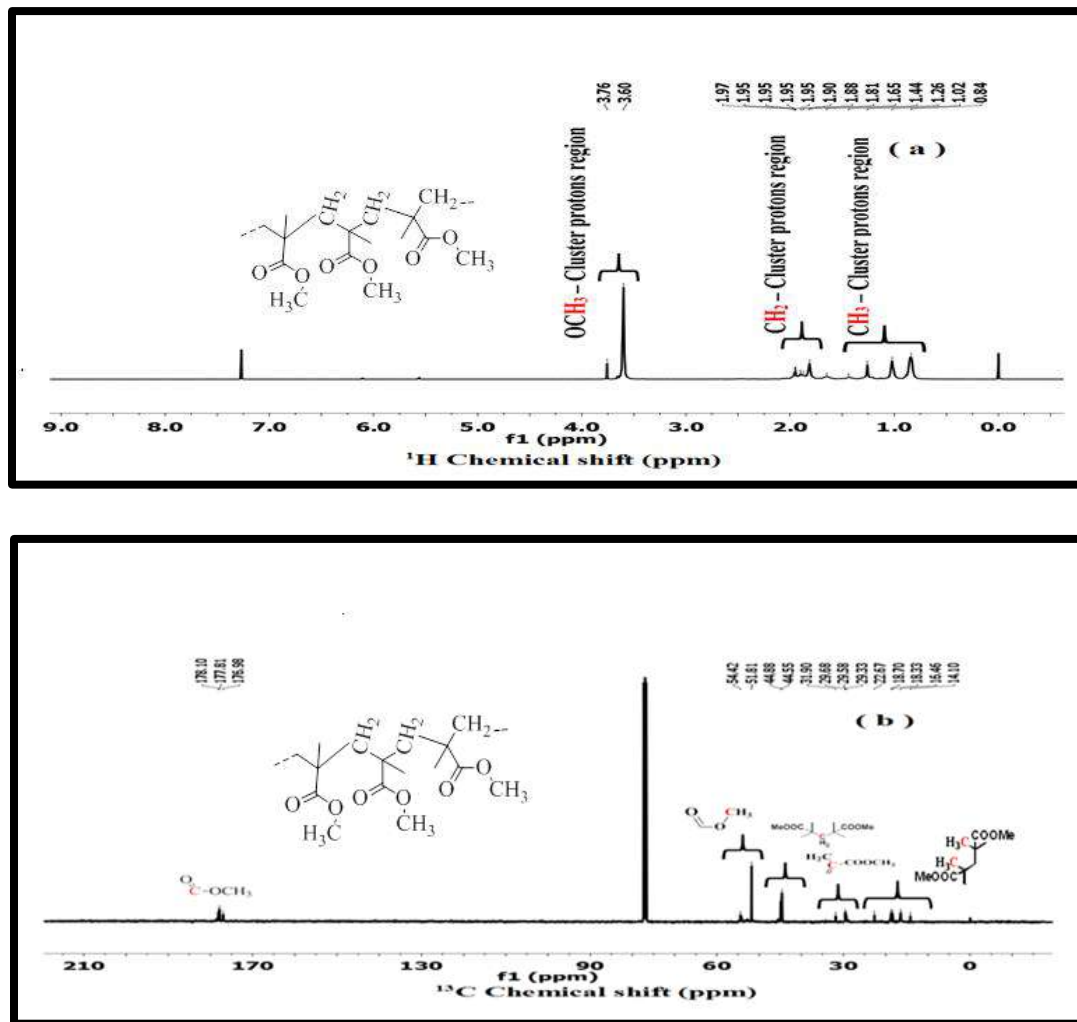


Fig 2a&2b: ¹H and ¹³C NMR Spectrum of PMMA

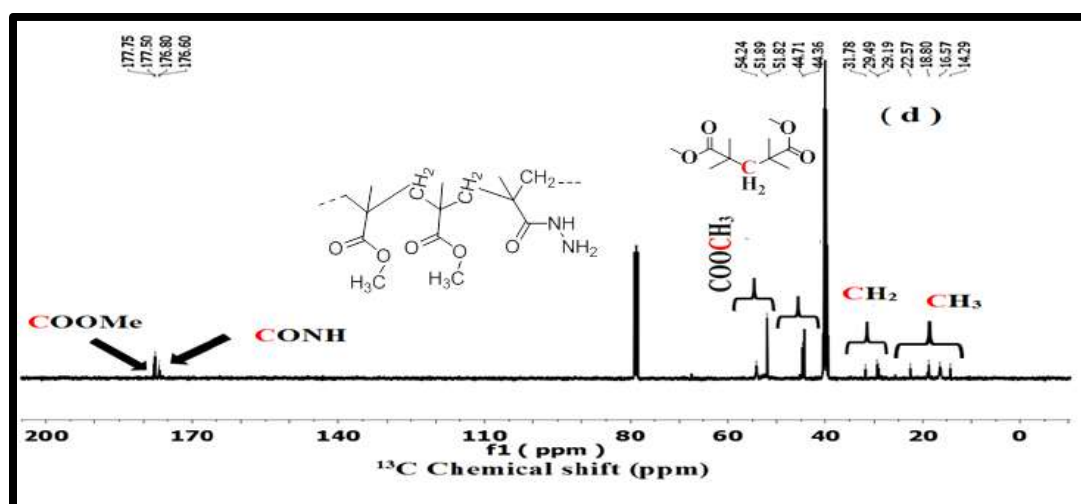
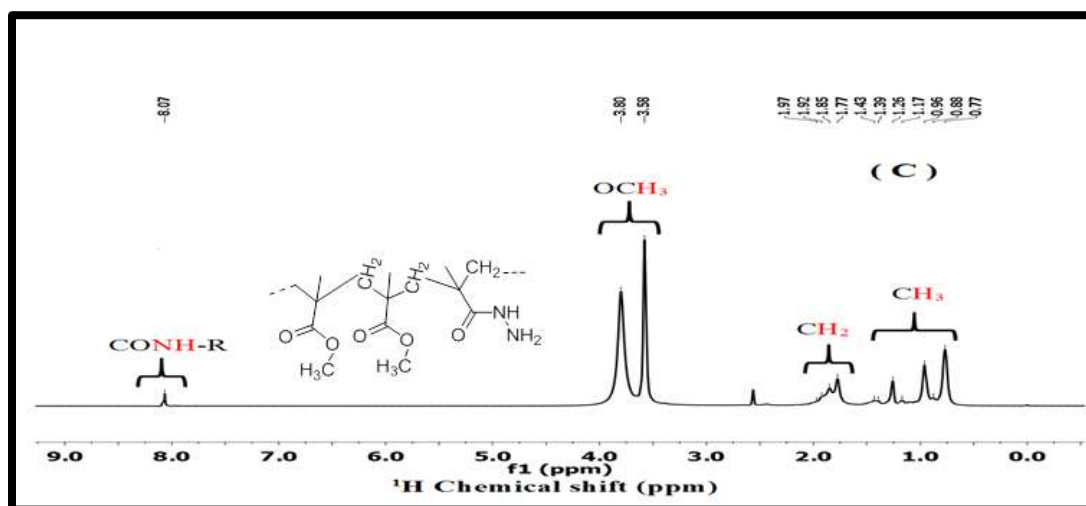
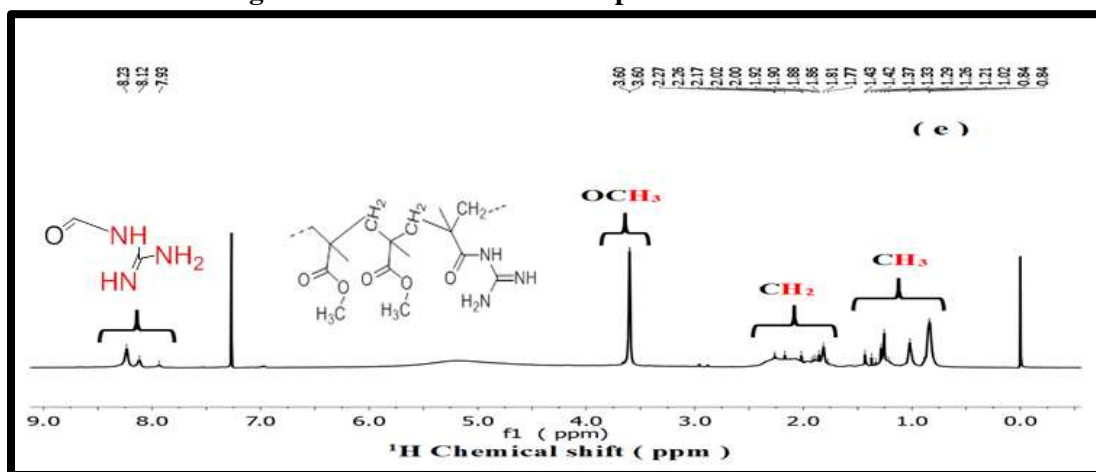


Fig 2c&2d: ^1H and ^{13}C NMR Spectrum of PMMA-H.



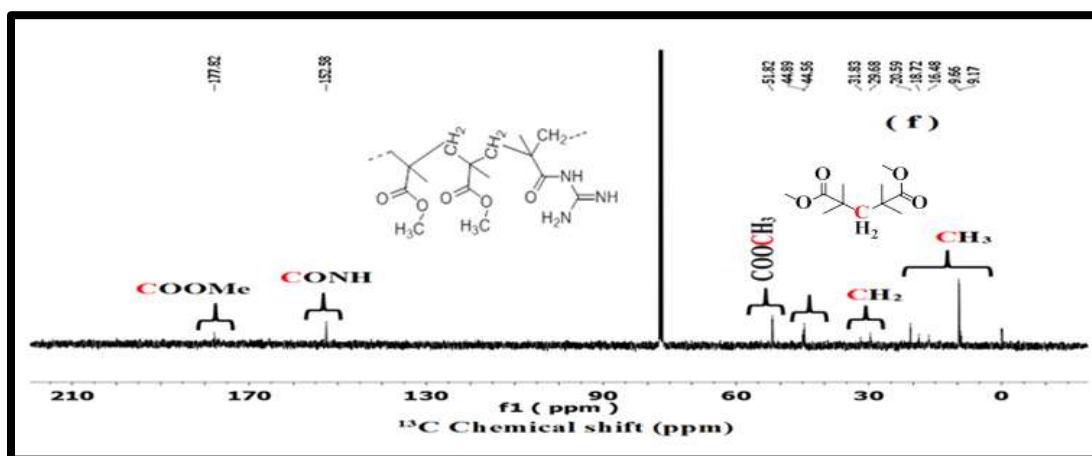


Fig 2e&2f: ^1H and ^{13}C NMR Spectrum of PMMA-G.

^1H and ^{13}C NMR spectral methods are used to confirm the structure of the modified linear polymers. The corresponding chemical shift values for hydrazide (CONH-NH₂) and (CONH-NH₂) quinidine amide linkages observed in proton NMR. The ^1H NMR of PMMA-H hydrazide^{11,12} linkage (fig 2c) showed at δ 8.07ppm for the N-H or amide proton, Peak value at δ 3.58ppm assigned for OCH₃,CH₂ proton assigned at δ 1.77ppm to 1.97ppm. Methylacrylate or CH₃ protons value at 0.77ppm to 1.43 ppm. The fig (2d) represented ^{13}C NMR spectra chemical shift value of ester carbon (COOCH₃) assigned 177.50ppm and 177.75ppm. Therefore amide carbon (CONH) 176.60 ppm and 176.80 ppm. Presence of peaks at 51.82ppm, 51.89ppm and 54.24ppm (COOCH₃). Peaks assigned at () carbon 44.36ppm and 44.71ppm. ^{13}C -NMR of PMMA-H hydrazide linkage: 29.19, 29.49, 31.78 ppm (CH₂), 14.29, 16.57, 18.80, 22.57ppm (CH₃). Showed (Fig 2e) ^1H NMR spectrum of PMMA-G quinuclidine amide linkage^{13,14} δ 7.93 to 8.23ppm (CONH-NH-NH₂), OCH₃ protons cluster assigned value 3.6 ppm, assigned CH₂ protons 1.77 to 2.27 ppm and CH₃ protons δ 0.84 to 1.43 ppm. ^{13}C NMR spectrum of PMMA-G (fig 2f) quinuclidine amide linkage (CDCL₃)

2.3.4 Gel permeation chromatography (GPC)

177.82 ppm (COOCH₃), 152.58 ppm (CONH), assigned 51.82ppm (COOCH₃), Carbon peak at δ () 44.56-44.89ppm, 29.68-31.83 ppm (CH₂), 9.17 to 20.59ppm (CH₃). The structural characteristics of modified PMMA-H and PMMA-G linear polymers were confirmed by ^1H and ^{13}C NMR

spectral studies.

2.3.3 Particle size & Zeta potential

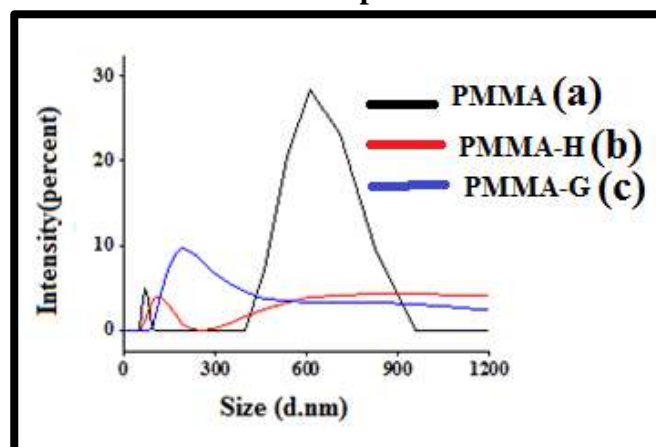


Fig 3: DLS analysis of Particle size distribution for (a) PMMA, (b) PMMA-H and (c) PMMA-G

The Z-average size distribution of PMMA and PMMA modified derivatives using DLS^{15,16} analysis was (Fig 3a,b,c) 710 ± 10 nm (PDI 0.5), 550 ± 10 nm (PDI 1.0), and 290 ± 10 nm (PDI 0.4) respectively with a negative zeta potential of -33.1, -25.5 and -7.2 mV, respectively.

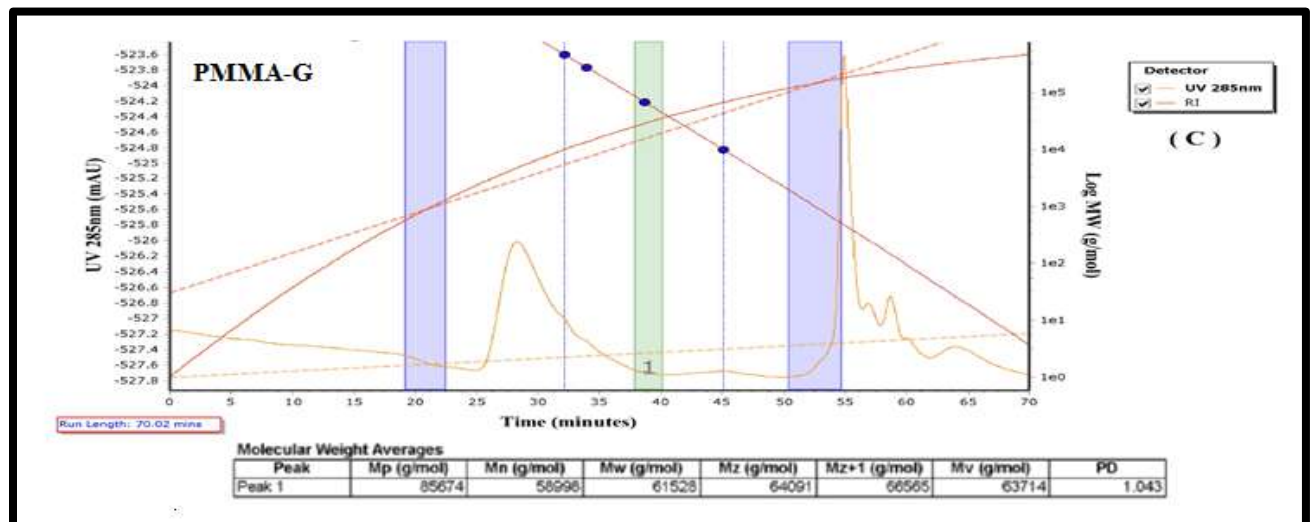
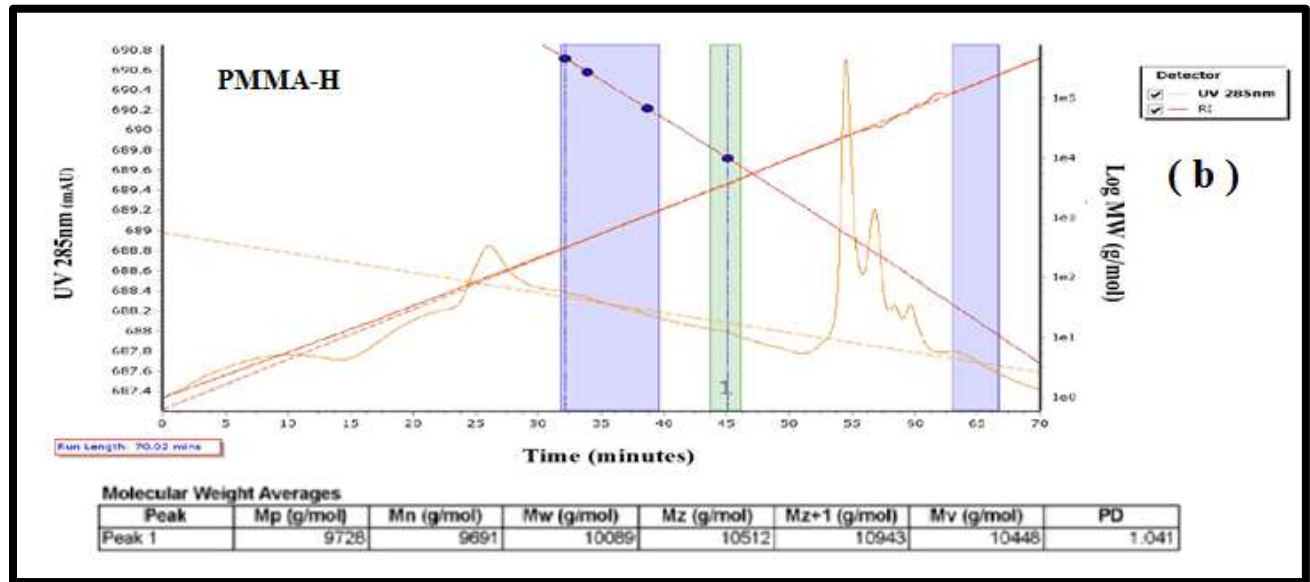
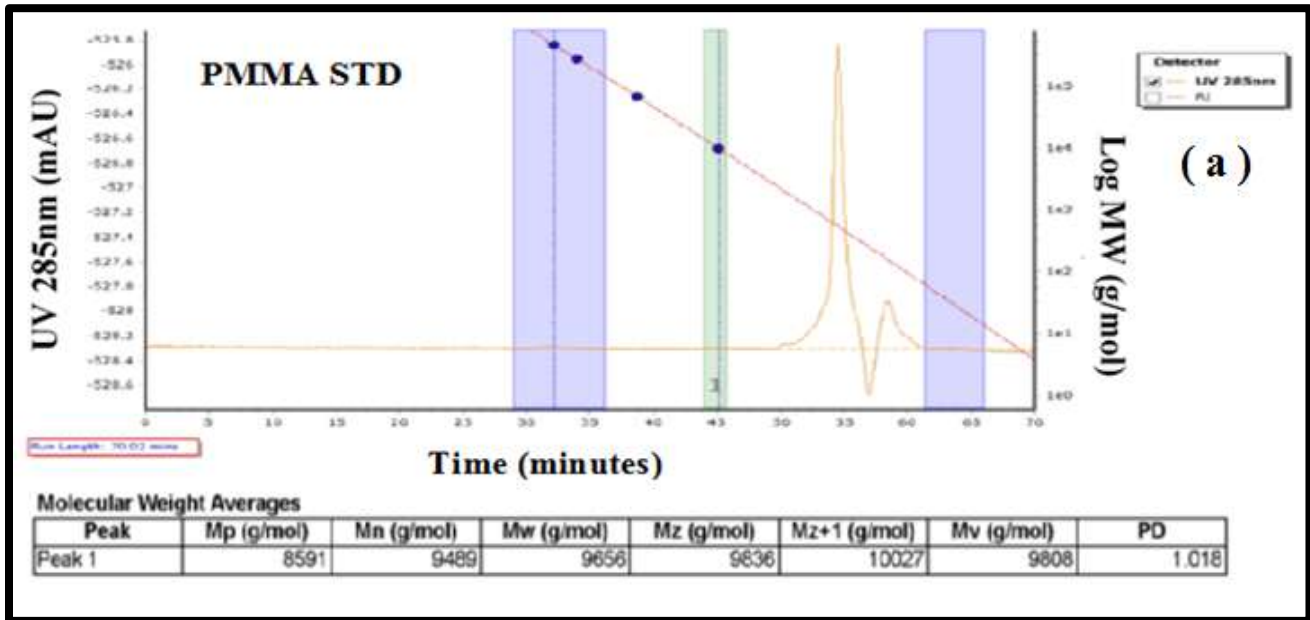


Figure 4. (a) GPC chromatogram of PMMA. (b) GPC chromatogram of PMMA-H. (c) GPC chromatogram of PMMA-G

GPC analysis of PMMA Weight average molecular weight 17-20 giving 9656 (M_w)⁻ (g/mol) and Number average molecular weight of 9489 (M_n)⁻ (g/mol) with polydispersity (PDI) of 1.018. Synthesized modified linear polymer average molecular weight of hydrazide 21-23 (PMMA-H) and amide guanidine (PMMA-G) 10089 (M_w)⁻ (g/mol), 9691 (M_n)⁻ (g/mol) and 61528 (M_w)⁻ (g/mol) 58998 (M_n)⁻ (g/mol) with polydispersity (PDI) of 1.041 and 1.043 respectively. The average molecular weight of the PMMA derivative was observed to be higher than that of the PMMA from the GPC results and shown in the Table-1.

Polymer	Weight Average Molecular Weight, $\overline{M_w}$	Number Average Molecular Weight, $\overline{M_n}$	PDI
PMMA	9656	9489	1.018
PMMA-H	10089	9691	1.043
PMMA-G	61528	58998	1.043

Table 1. GPC results for the PMMA and PMMA derivatives polymer. (M_w)⁻, average-weight molecular weight; (M_n)⁻, average-number molecular weight; PDI, polydispersity index.

2.3.5 Differential scanning calorimetry (DSC)

Thermal analysis techniques such as DSC are generally employed to analyse the thermal characteristics such as melting temperature (T_m) and glass transition temperature (T_g). The T_g depends on the molecular mobility of materials in crystalline as well as amorphous structures. The DSC thermo gram of (Fig 4&5) PMMA shows T_g at 45.44°C and an endothermic curve ~ 84.39 °C. The T_g corresponding to PMMA-modified derivatives like guanidine amide decreases

to T_g at 40.75°C but did not reveal DSC shows hydrazine T_g and the broad endothermic curve obtained from the graph at 105.64°C. Typical DSC curves of guanidine hydrazide heat transition of endothermic temperature at 123.03°C and 220.58°C respectively. In DSC thermogram, the glass transition of modified polymers values is comparatively lower than the T_g of the pure PMMA. All the polymers degradation starts from ~300°C.

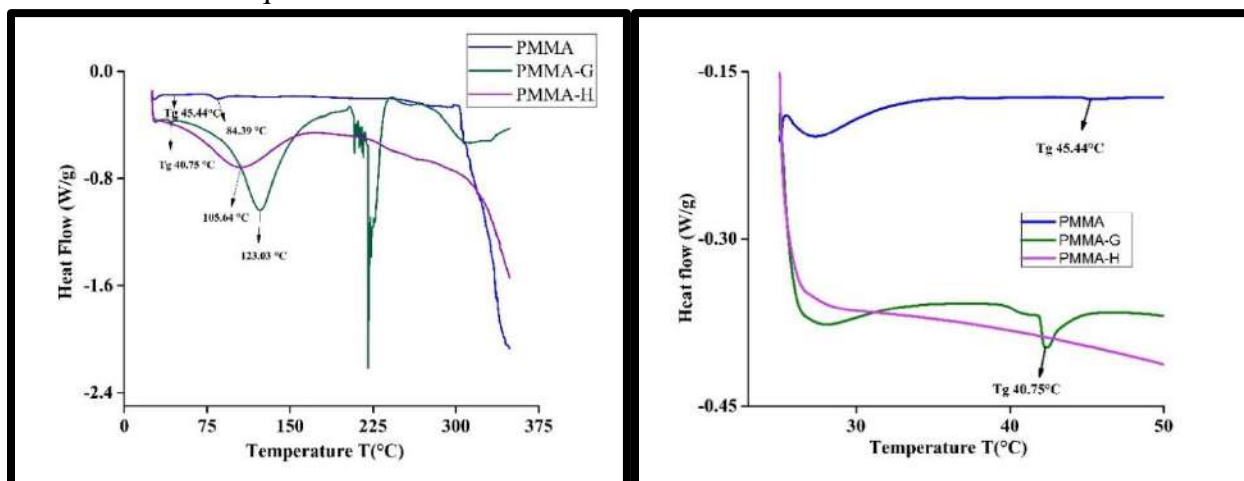


Figure 5 and 6. DSC curves of PMMA and PMMA derivatives at a heating rate of 5 °C/min in nitrogen.

The increased melting temperature of modified polymers is higher than PMMA. Data proved that modified polymers thermally stable than PMMA. The reason for phase, changes confirm by the endothermic temperature values of the aliphatic-modified hydrazide polymers compound.

2.3.6 Thermogravimetric Analysis (TGA)

The thermal stability of PMMA and PMMA modified polymers was investigated by TGA and shown in Fig.7. From the thermograph a single-step degradation²⁷ was observed in PMMA, which began at about 288 °C and

finished at about 425 °C. It can be seen from the graph undergoes one major stage of degradation in this temperature and the value of the weight loss at this stage is 94.63%. There was a negligible weight loss (2–4%) up to 100 °C, which might be due to the moisture present on the samples. The ash content (at 800 °C) of pure PMMA was 1.57% and total weight loss 98.43%. Hydrazine hydrazide PMMA-H compound, TGA curve showed two steps of thermal degradation occurred.

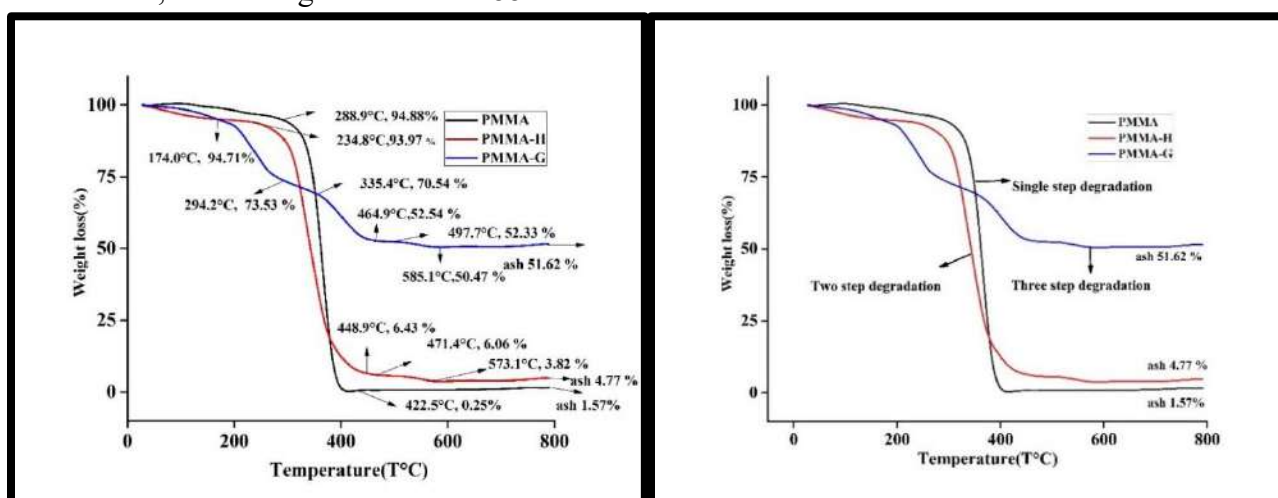


Figure 7. TGA curves illustrate the thermal degradation temperature of the PMMA compared to PMMA modified compounds.

First degradation temperature from 234.8°C to 448.9°C with the weight loss of 87.54% and second degradation temperature from 471.4°C to 573.1°C with the weight loss of 2.24%. Ash content 4.77% and total loss of mass value 95.23%. Modified PMMA compound like PMMA-G, TGA curve indicated three stage of degradation was observed. First stage of decomposition temperature starts from 174.0°C and ends at 294.2°C with sum of weight loss 21.18%. Second degradation steps starts from 335.4°C and ends at 464.9°C and % of

weight loss in this stage at 18%. Third degradation temperature starts from 497.7°C to 585.1°C with mass loss value 1.86%. After decomposition residue content 51.62%. Total weight loss 48.38%.

2.3.7 FE-SEM (Field emission scanning electron microscopy)

The surface morphological of PMMA sample and after chemical modification of the PMMA samples in the present study were analyzed using FESEM analysis.

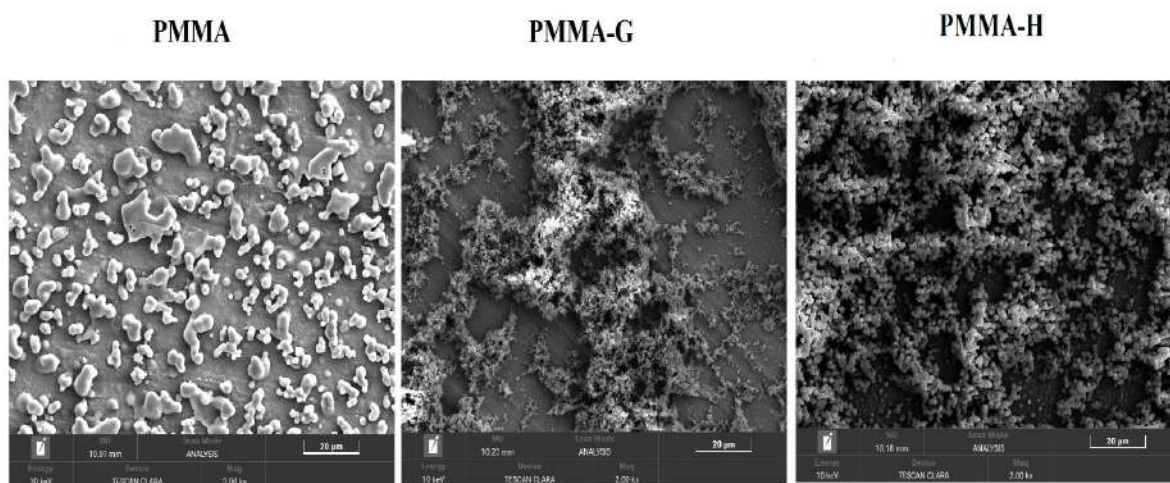


Figure 6. Morphological features of FE-SEM images PMMA, PMMA-G, and PMMA-H

2.4 Antimicrobial studies

2.4.1 Antibacterial studies

Materials

Standard cultures for antimicrobial assays were stepped up from Microbial Type Culture Collection (MTCC), IMTECH, Chandigarh, India.

The agar well diffusion method³¹ was performed to determine the anti-microbial activity of the synthesized polymerized materials. These organisms namely Gram +ve (*Bacillus cereus* (MTCC 4079), *Staphylococcus aureus* (MTCC 737), Gram -ve (*Escherichia coli* (MTCC 1687), *Pseudomonas aeruginosa* (MTCC 1688). Fresh overnight (24hrs) bacterial culture (1×10^5 cells/mL) was spread evenly on the surface of nutrient agar with the help of cotton swabs. Then, with a sterile cork borer, holes of 6 mm were punctured. Varying volumes (25-75µl) of compounds were loaded aseptically into the holes, and the plate was incubated for 24 hrs. Ampicillin was used as the positive control 32-35.

2.4.2 Cell viability by MTT assay

The Lung cancer cell lines of A549 seeded in 96-well micro plates (1×10^6 cells/well) and incubated at 37°C for 24 h in 5% CO₂ incubator and allowed to grow 95%

confluence. Then the medium was replaced and the cells were treated with and PMMA sample and modified basis compounds PMMA-G and PMMA-Hat different concentration of such as 10, 20, 30, 40 and 50 µg/mL and incubated for 24 h. The cells were then washed with phosphate-buffer saline (PBS, pH- 7.4) and 20 µL of (MTT) solution (5 mg/mL) was added to each well. The plates were then stand at 37°C in the dark for additional 4 hr. The formazan crystals were dissolved in 100 µL DMSO and the absorbance was read spectrometrically at 570 nm. The percentage of cell viability was expressed as formula.

$$\text{Cell viability (\%)} = \frac{\text{OD absorbance treated cell}}{\text{OD absorbance of control cell}} \times 100$$

The concentration that inhibited 50% of cell growth was referred as IC₅₀ value, which was used as a parameter for cytotoxicity study. The morphological changes of untreated (control) and treated cells were observed under the FLoId Cell Imaging Thermo Fisher –Invitrogen EVOS XL Model after 24 h and photographed.

2.4.3 Apoptosis assay of Modified PMMA compounds

Cell apoptosis was examined using Venugopal et al.'s (2017) protocol³⁶. Acridine orange/propidium iodide (AO/PI) staining served as a useful method for identifying cell growth. Using the minimum inhibitory strength of modified PMMA identified by the MTT assay, A549 cancer cells were seeded in 96-well plates and incubated for 24h. Following treatment, 5 μ L of a fluorescent dye stain (acridine orange, 100 μ g/mL) and 5 μ L of propidium iodide (PI, 100 μ g/mL) were added to the treated cells and washed with phosphate buffer saline. When AO dye binds to both viable and nonviable cells, it emits either red or green fluorescence; in contrast, PI emits only red fluorescence when it connects to nonviable cells. The morphological changes^{37,38} in the apoptotic nuclei (intensely stained, fragmented nuclei and condensed chromatin) cells were observed using a Fluorescent Cell Imaging microscope.

RESULT AND DISCUSSION

For the purpose of characterization of modified PMMA derivatives, FT-IR, ¹H and ¹³C NMR spectra were recorded. The commercial sample (Sigma –Aldrich) of PMMA was used for recording spectra. The proton NMR spectra (Fig 2a) of PMMA show two ester, two methylene, and two methyl signals. The ¹³C –NMR spectrum (Fig 2b) displays two ester signals & clusters of ¹³C signals corresponding –CH₂- & -CH₃ groups. In the FT-IR spectrum (Fig 1a) of PMMA, a strong stretching at 1732 cm⁻¹ confirms the presence of the ester group. Stretching vibrations corresponding to CH₃ and CH₂ moieties are also a distinct in the FT-IR spectrum. These spectral characteristics are useful to confirm the modification of PMMA upon reaction with hydrazine and guanidine. When PMMA is modified with NH₂-NH₂, in addition to the ester signals (at 3.58 & 3.80 ppm), a new signal appears

at 8.07 ppm, corresponding to the newly formed amide bond (hydrazide bond). The formation of the hydrazide derivative of PMMA is confirmed by the additional ¹³C resonances in the range of 176.60-177.75 ppm. The presence of a free amino group was also confirmed through the Ninhydrin Test (...development of purple color). Encouraged by these results, we attempted to obtain PMMA derivatives modified with hydrazine and guanidine amide. As expected, the guanidine derivative of PMMA showed three resonances at ~ 7.93, 8.12, 8.23 ppm corresponding to newly formed CO-NH bond. Partial modification of PMMA is evident from the appearance of a singlet at 3.60 ppm stemming from the residual ester group (COOMe). The ¹³C NMR spectrum shows the presence of ester carbonyl 177.82 ppm and amide carbonyl 152.58 ppm moieties. Partial modification of PMMA by guanidine is supported by the FT-IR data (Fig 1b), which shows both ester and amide stretching vibrations at 1732 cm⁻¹ and 1668 cm⁻¹, respectively. In DLS analysis, the modified linear polymers like hydrazide derivative of PMMA guanidine (PMMA-G) and hydrazine (PMMA-H) showed (Figure 3) less particle size than the (PMMA) due to their aliphatic hydrazide moiety formation. The higher negative zeta potential denoted the strong repulsion force between the particles causing an amplification or enhancement of stability. The DLS measurement of PMMA was negative in charge with a zeta potential value higher than the PMMA modification compounds. For the data evidence, a higher zeta potential charge would lead to a long time storage stability of the PMMA compared to PMMA derivatives (Raja et al. 2015; Varadavenkatesan et al. 2016). The glass transition temperature of unmodified pure PMMA has a somewhat higher value than that of modified linear compounds, as seen by the DSC curve in the graphs (Figures 5 and 6). However, the DSC graph was ensured by exothermic temperature, which is



the melting point temperature at which PMMA-G and PMMA-H had higher values due to modified compounds' phase transitions at varying temperatures. According to data, modified PMMA (PMMA-G, PMMA-H) has higher melting temperature corresponding to thermal stability than PMMA. It is evident that the PMMA and derivative compounds exhibited different thermal degradation behaviors. The modified compound's TGA degradation temperature starts earlier and higher degradation temperature corresponding to it is noticed in the lower and high values of ash content (1.57%) for PMMA and (4.77% and 51.62%) for modified polymer (PMMA-H) is slightly higher and more values as (PMMA-G) compounds. The possible explanation for the higher thermal stability of the modified polymer in comparison with the PMMA is that, during thermal degradation, the polymer degrades rapidly

and leads to the formation of hydrazide or amide moiety, which may be more stable in comparison with the PMMA. Average molecular weight of the PMMA derivative was observed to be higher than that of the PMMA from the GPC results. PMMA modified of two compounds average molecular weight confirm by the GPC data (Figure 4). The surface and size of the PMMA was observed from the images to compare after the chemical polymerization of modified compounds was changed. This morphological changes supported the biological activities of the modified PMMA-G and PMMA-H in the present research work. FE-SEM39-41 images showed the morphology of PMMA-G and PMMA-H were smaller in size and further the molecule were aggregated to each other in compare to PMMA.

3.1 Anti-bacterial activity

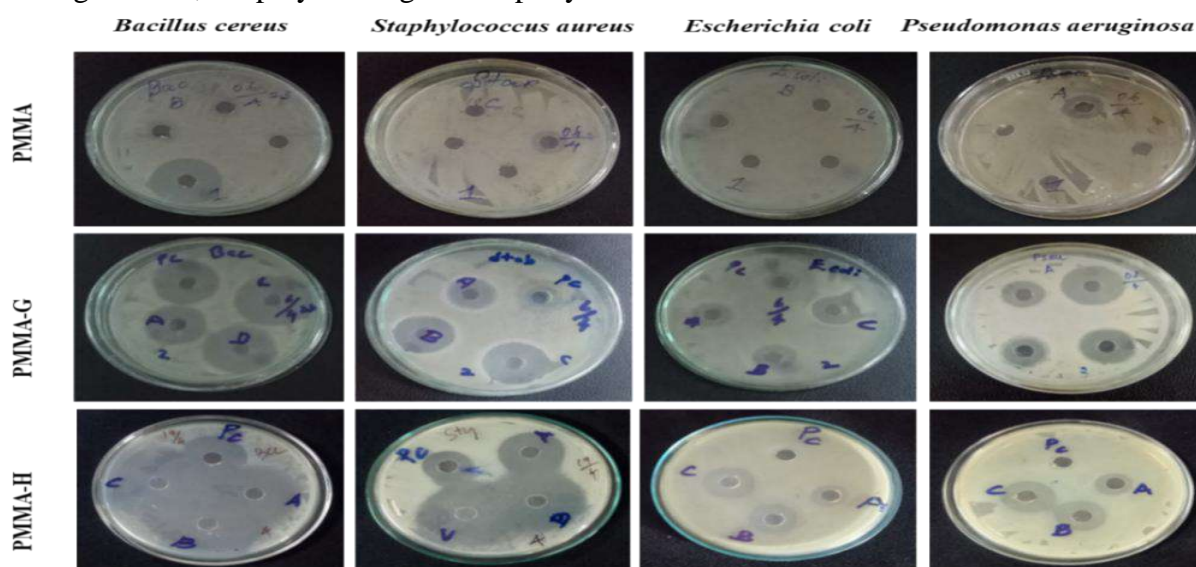


Figure 7. PMMA, PMMA-G and PMMA-H treated with gram positive and gram negative bacteria

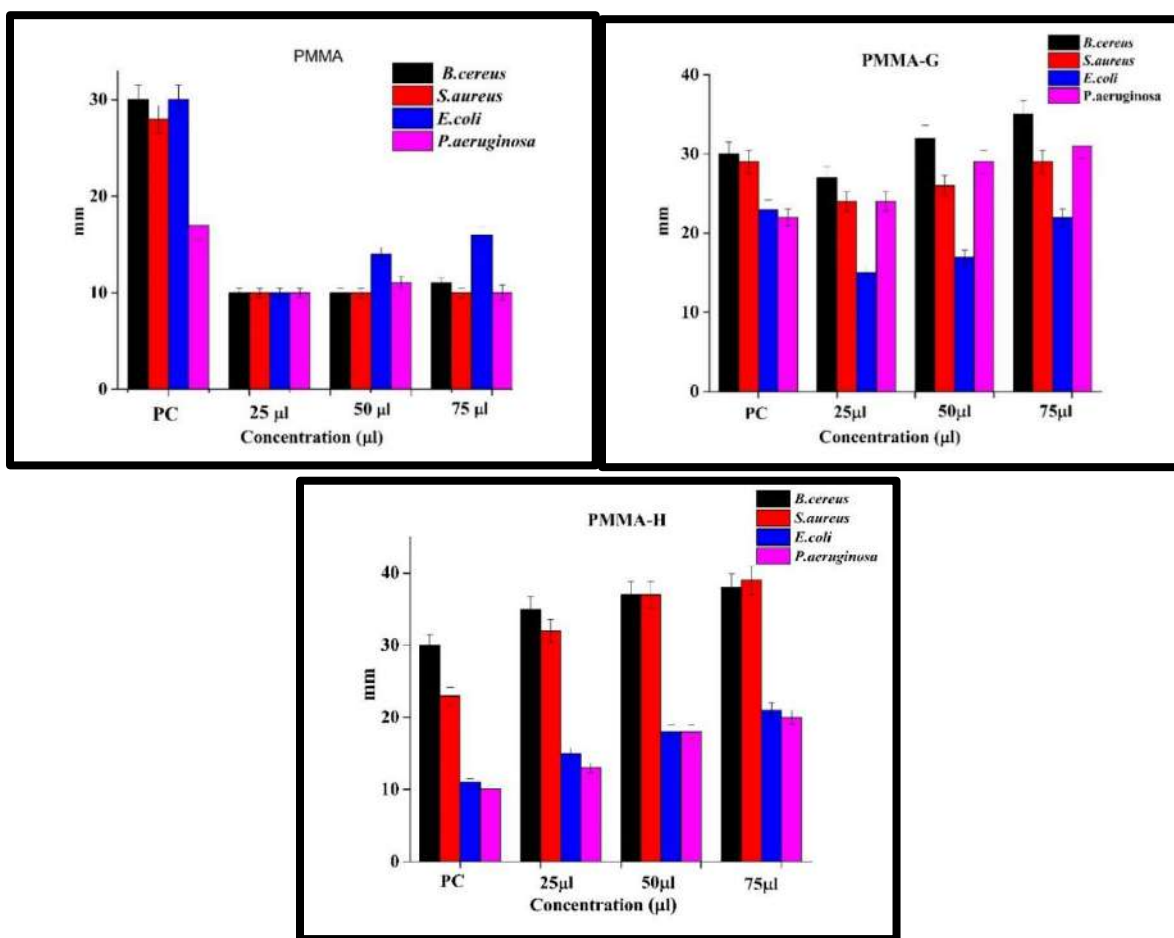


Figure 8. Antibacterial activity of PMMA, PMMA-G, and PMMA-H

Both the direct and indirect role occurs in a parallel system, making these compounds an excellent tool to combat the above microbes. This study worked to assess the efficiency of the synthesized polymerized materials towards both gram + ev and gram -ev bacteria with the highest concentration of approximately 106 CFU/mL. Among three compounds, PMMA was found to have the least effective zone of inhibition because its incorporating free amino and hydrazide or amide groups into PMMA made it possible to synthesize modified linear polymers with improved hydrophilicity, better solubility in aqueous media, and solubility in organic solvents. This modified linear polymer also allowed for the protonation of the free amino and hydrazide groups, which improved their

antibacterial activity. Whereas PMMA-G linear polymer and PMMA-H provide a maximum zone of inhibition due to their hydrazide and amide moiety in the modified linear polymer of basic compounds.

3.2 Anticancer activity of PMMA-modified compounds against A549 cell line

The lung cancer cell line (A549) was used to test the PMMA standard and modified compounds' anticancer activity. The results are shown in Figure 9. The MTT assay was carried out by exposing A549 cells to different concentrations (10–50 µg/mL) of PMMA std, PMMA-G, and PMMA-H for 24 hours. The treated and untreated cells were analyzed for morphological changes and cell viability in the PMMA standard and PMMA-modified samples. According to the results, compared to

untreated cells, the growth of cancer cells was marginally decreased by an increase in PMMA concentration.

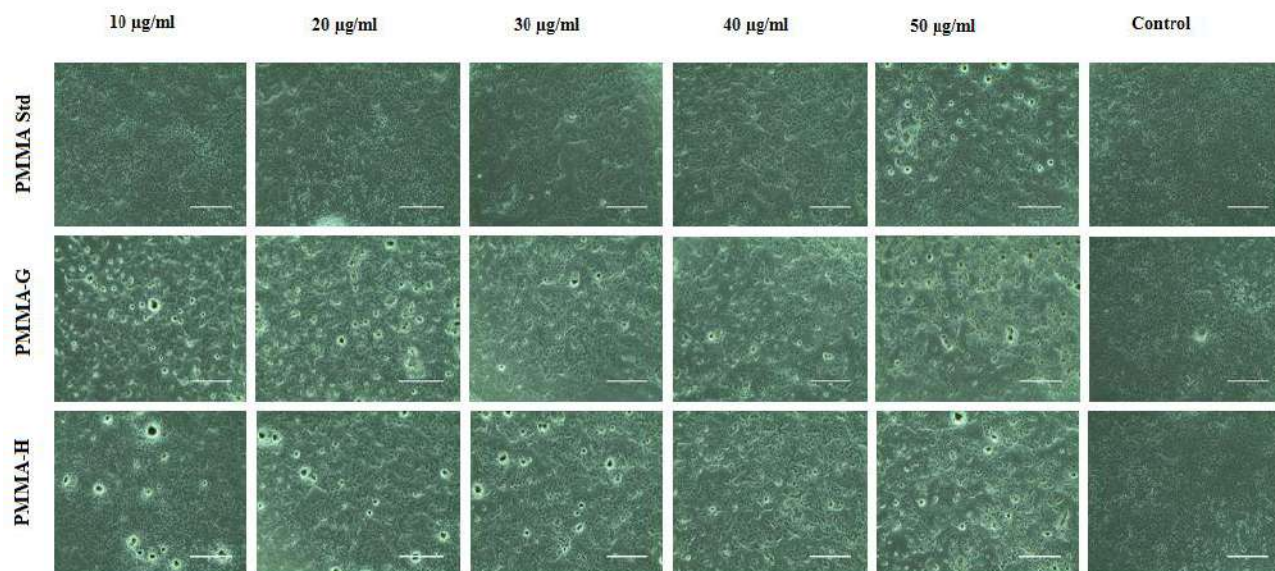


Figure 9. Optical microscopic images showing the apoptosis of A549 lung cancer cells treated with standard PMMA and the modified PMMA-G and PMMA-H.

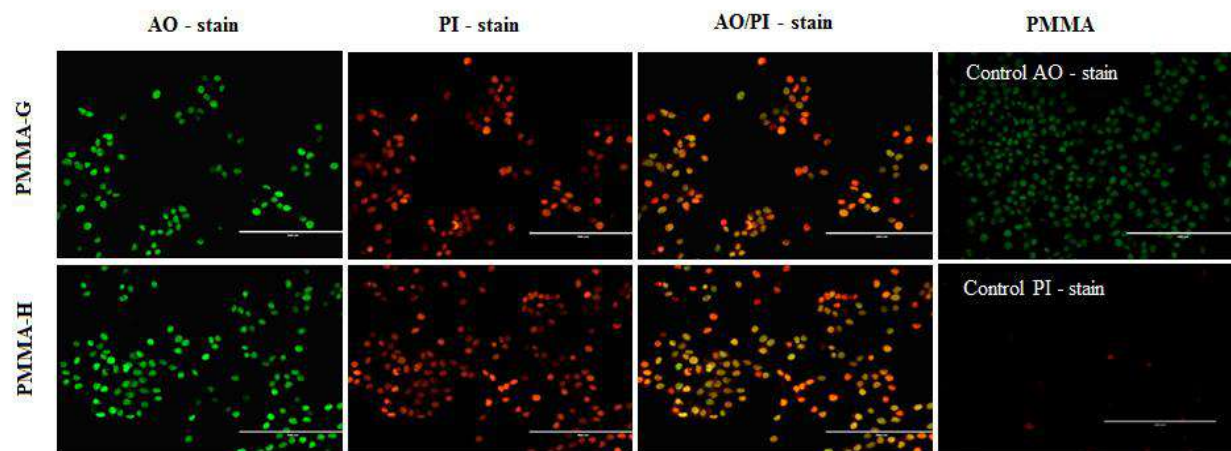


Figure 10. The fluorescence microscopy images show the dual AO/PI staining assay-based apoptosis in A549 lung cancer cells.

The results of modified compounds indicated a significant decrease in cancer cell proliferation (10–50 µg/ml) as compared to untreated cells. With five different concentrations of PMMA-G and PMMA-H, a wide range of cell viability was inferred. The maximum decrease in cell viability was witnessed at 50 µg/mL (IC₅₀) compared to the PMMA standard, as inadequate cell viability was shown in the microscopic images (**Figure 9**) It is

verifiable that the compounds PMMA-G and PMMA-H can kill cancer cells.

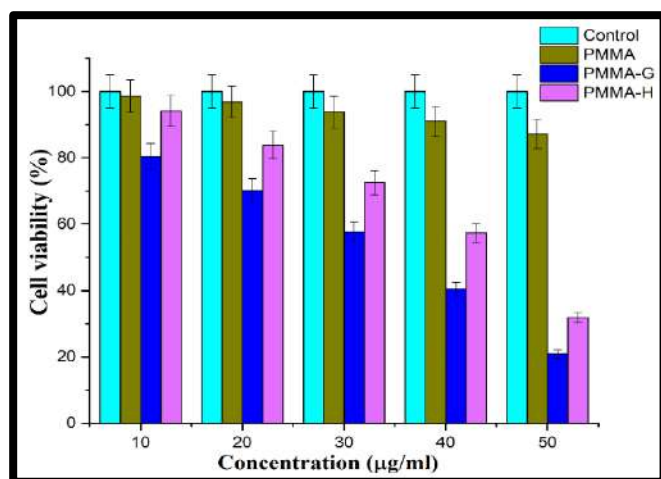


Figure 11. Anticancer activity test results of PMMA modifies.

According to the images, at low concentrations, both compounds moderately kill cancer cells, ranging from 10 to 50 µg/mL, (Figure 11) and at higher concentrations of both substances, kill cancer cells. In the MTT experiment, the PMMA showed 87% cell viability and 13% anticancer activity against lung cancer A549 cells. PMMA-G, a modified polymeric molecule, exhibited anticancer activity 79% of cancer cells and 21% of cell viability. In PMMA-H, the anticancer activity against cancer cells was 68%, whereas the cell viability was 32%. Anticancer activity is less for PMMA compared to PMMA-G and PMMA-H from the evidence for the microscopic image in the MTT assay result. An apoptosis experiment using dual AO/PI labeling was used to establish the anticancer activity further; the resulting data are displayed in Figure 10. The PMMA demonstrated a very less level of apoptosis as measured by the emission of minute red cells, or dead cells, as a result of poor protein binding, low cell affinity, and nuclear membrane contact. Comparing the PMMA-G and PMMA-H to the PMMA, the apoptosis assay revealed greater results. Both readily attach to DNA, which causes chromatin condensation, DNA fragmentation, and a change in cell shape. Therefore, in comparison to the PMMA (uniform bright green nuclei and cytoplasm), the A549

Lung cell line treated with these PMMA-G and PMMA-H generated a maximum amount of red fluorescence (late apoptosis or necrosis) with round-shaped morphology. These results suggest that PMMA-G and PMMA-H, both modified polymeric compounds, have better anticancer activity against cancer cells than normal cells. According to the modified compounds' anticancer effect, the hunt for alternative chemotherapeutic drugs may benefit from their contributions.

CONCLUSION

In this investigation, guanidine and hydrazine incorporated PMMA were designed and synthesized for biological applications. All the analytical-related data such as FTIR, NMR, GPC, thermal analysis and FESEM, etc., supported and confirmed the formation of amide guanidine and hydrazide moiety in the modified polymers. The antibacterial activity of these modified polymeric compounds was significantly better than that of the distinct PMMA. According to the findings, the surface morphology, particle size, and concentration of hydrazide modification of PMMA derivatives have significant impact on the bacterial inhibitory mechanism. They are more effective against both gram-positive and gram-negative bacteria. According to the test results, the prepared PMMA modified polymeric materials possess potential anticancer capacity and implant for controlled drug release.

REFERENCE

1. Nadia A. Mohamed & Nahed A. Abd El-Ghany. Synthesis, characterization, and antimicrobial activity of chitosan hydrazide derivative. *International Journal of Polymeric Materials and Polymeric Biomaterials*, 66:8,410-415, DOI: 10.1080/00914037.2016.1233419.
2. Zhongshan Liu, Junjie Ou, Hongwei Wang, Xin You and Mingliang Ye. Synthesis and

- Characterization of Hydrazide-Linked and Amide-Linked Organic Polymers. *ACS Appl. Mater. Interfaces* 2016, 8, 32060–32067. DOI: 10.1021/acsami.6b11572.
- GavhaneYogeshkumar, N.; GuravAtul, S.; YadavAdhikrao, V. *Int. J. Res. Pharm. Biomed. Sci.* 2013,4,312
 - HaofengQiu, Zhangyong Si, Yang Luo, Peipei Feng, Xujin Wu, WenjiaHou,Yabin Zhu, Mary B. Chan-Park,LongXu and Dongmei Huang,The Mechanisms and the Applications of Antibacterial Polymers in Surfacepublished: 11 November2020doi: 10.3389/fbioe.2020.00910.
 - Allison, B. C., Applegate, B. M., and Youngblood, J. P. (2007). Hemocompatibility of hydrophilic antimicrobial copolymers of alkylated 4-vinylpyridine. *Biomacromolecules* 8, 2995–2999. doi: 10.1021/bm7004627.
 - Li, M., Mitra, D., Kang, E. T., Lau, T., Chiong, E., and Neoh, K. G. (2017).Thiol-ol chemistry for grafting of natural polymers to form highly stable and efficacious Antibacterial Coatings. *ACS Appl. Mater. Interfaces* 9, 1847–1857.doi: 10.1021/acsami.6b10240.
 - Vicini, P.; Geronikaki, A.; Incerti, M.; Busonera, B.; Poni, G.; Kabras, C. A.; Colla, P. L. *Bioorg. Med. Chem.* 2003, 11, 4785.
 - Ravi Kumar, M. N. V.; Muzzarelli, R. A. A.; Muzzarelli, C.; Sashiwa, H.; Domb, A. J. *Chem. Rev.* 2004, 104, 6017.
 - Ravi Kumar, M. N. V. *React. Funct. Polym.* 2000, 46, 1.
 - Sztanke, K.; Maziarka, A.; Sztanke, M. *Bioorg. Med. Chem.* 2003, 21, 3648.
 - M. R. Menyashev, A. I. Martynenko, N. I. Popova, N. A. Kleshcheva, and N. A. Sivov.Guanidine Methacrylate and Methacryloyl Guanidine Hydrochloride:Synthesis and Polymerization. *Polymer Science, Series B*, 2016, Vol.58, No. 5, pp. 556–563 DOI: 10.1134/S1560090416050080.
 - N. A. Sivov, *Biocide Guanidine SontainingPolymers:Synthesis, Structure and Properties* (Brill AcademicPubl., Leiden, 2006).
 - Martynenko, A.I.; Khashirova, S.Y.; Malkanduev, Y.A.; Sivov, N.A. *Guanidine-Containing Monomers and Polymers: Synthesis,Structure, Properties*, 1st ed.; Izd M. and V. Kotlyarovyh: Nalchik, Russia, 2008; p. 232.
 - Menyashev, M.R.; Martynenko, A.I.; Popova, N.I.; Kleshcheva, N.A.; Sivov, N.A. *Guanidine Methacrylate and methacryloyl guanidine hydrochloride: Synthesis and polymerization.* *Polym. Sci. Ser. B* 2016, 58, 556–563.
 - Samarth Bhargava,Justin Jang Hann Chu,and Suresh Valiyaveetil. Controlled Dye Aggregation in SodiumDodecylsulfate-Stabilized Poly (methylmethacrylate) Nanoparticles as Fluorescent Imaging Probes. *ACS Omega* 2018, 3, 7663–7672. DOI: 10.1021/acsomega.8b00785.
 - S. Vasantharaja, N. Sripriya, M. Shanmugavel, E. Manikandan, A. Gnanamani,P Senthilkumar.Surface active gold nanoparticles biosynthesis by new approach for bionanocatalytic activity.*Journal of Photochemistry & Photobiology, B: Biology* 179 (2018) 119–125. doi.org/10.1016/j.jphotobiol.2018.01.007.
 - K. Kasinathan, J. Kennedy, E. Manikandan, M. Henini, M. Maaza, Photodegradation of organic pollutantsRhB dye using UV simulated sunlight on ceria based TiO2

- nanomaterials for antibacterial applications, *Sci. Rep.* 6 (2016) 38064.
18. Miao, M.; Chen, Q.; Zhang, C.; Cao, X.; Zhou, W.; Qiu, Q.; An, Z. Nanoprecipitation of PMMA Stabilized by Core Cross-Linked Star Polymers. *Macromol. Chem. Phys.* 2013, 214, 1158–1164.
 19. Morales-Cruz, M.; Flores-Fernández, G. M.; Morales-Cruz, M.; Orellano, E. A.; Rodriguez-Martinez, J. A.; Ruiz, M.; Griebenow, K. Two-step nanoprecipitation for the production of protein-loaded PLGA nanospheres. *Results Pharma Sci.* 2012, 2, 79–85.
 20. Praveen C. Ramamurthy, Ashwini N. Mallya, Alex Joseph, William R. Harrell, Richard V. Gregory. Synthesis and Characterization of High Molecular Weight Polyaniline for Organic Electronic Applications. *POLYMER ENGINEERING AND SCIENCE*—2012. DOI 10.1002/pen.
 21. Williams G. Skene and Jean-Marie P. Lehn. Dynamers: Polyacylhydrazones reversible covalent Polymers, Component exchange, and constitutional diversity. *PNAS* June 1, 2004 vol. 101 no. 22 www.pnas.org/cgi/doi/10.1073/pnas.0401885101.
 22. Lehn, J.-M. (2002) *Proc. Natl. Acad. Sci. USA* 99, 4763–4768.
 23. Cousins, G. R. L., Poulsen, S. A. & Sanders, J. K. M. (2000) *Curr. Opin. Chem. Biol.* 4, 270–279.
 24. NidalWanisElshereksi, Saied Hamd Mohamed, AzlanArifin and ZainalArifinMohd Ishak. Thermal Characterisation of Poly (Methyl Methacrylate) Filled with Barium Titanate as Denture Base Material *Journal of Physical Science*, Vol. 25(2), 15–27, 2014.
 25. McCabe, J. F. & Walls, A. W. G. (2008). *Applied dental materials*, 9th ed. London: Blackwell.
 26. Hergeth, W. et al. (1989). Polymerization in the presence of seeds. Part IV: Emulsion polymers containing inorganic filler particles. *J. Polym.*, 30, 254–258.
 27. Ash, B. J., Schadler, L. S. & Siegal, R. W. (2002). Glass transition behavior of alumina/polymethylmethacrylate nanocomposites. *J. Mater. Lett.*, 55, 83–87.
 28. M. Schneider, T. Pith, and M. Lambla, “Impact modification of thermoplastics by methyl methacrylate and styrene-grafted natural rubber latexes,” *Polymers for Advanced Technologies*, vol. 6, no. 5, pp. 326–334, 1995.
 29. S. Jun-Yeob, K. Jin-Woong, and S. Kyung-Do, “Poly(methyl methacrylate) toughening with refractive index-controlled core-shell composite particles,” *Journal of Applied Polymer Science*, vol. 71, no. 10, pp. 1607–1614, 1999.
 30. Eastmond, G. C.; Paprotny, J. *React Funct Polym* 1996, 30, 27.
 31. V. Manikandan, P. Velmurugan, J. H. Park, W. S. Chang, Y. J. Park, P. Jayanthi, B. T. Oh, Green Synthesis Of silver oxide nanoparticles and its antibacterial activity against dental pathogens, *3 Biotech*, 7(1), (2017)1-9. <https://doi.org/10.1007/s13205-017-0670-4>.
 32. Ana Maria Carmona-Ribeiro and Péricles Marques Araújo. Antimicrobial Polymer Based Assemblies: A Review. *Int. J. Mol. Sci.* 2021, 22, 5424. <https://doi.org/10.3390/ijms22115424>
 33. Nadia A. Mohamed & Nahed A. Abd El-Ghany. Synthesis, characterization, and antimicrobial activity of chitosan hydrazide derivative, *International Journal of Polymeric Materials and Polymeric Biomaterials*,

- 66:8,410-415, DOI: Hasan, R. K. Asthana, *J. Drug Deliv. Sci. Tec.* 2019, 51, 164.
10.1080/00914037.2016.1233419
34. Xueli Sun, Zhiyong Qian, Lingqiong Luo, †Qipeng Yuan, Ximin Guo, Lei Tao, Yen Wei, and Xing Wang, *ACS Appl. Mater. Interfaces* 2016, 8, 28522–28528. DOI: 10.1021/acsami.6b10498.
35. Kumar LV, Naik PJ, Khan PS, Reddy AB, Sekhar TCh, Swamy GN (2011a) Synthesis, characterization and biological evaluation of some new hydrazide hydrazones. *Der Pharm Chem* 3(3): 317–322.
36. K. Venugopal, H.A. Rather, K. Rajagopal, M.P. Shanthi, K. Sheriff, M. Illiyas, M. Maaza, Synthesis of silver nanoparticles (Ag NPs) for anticancer activities (MCF 7 breast and A549 lung cell lines) of the crude extract of *Syzygium aromaticum*, *J. Photochem. Photobiol. B Biol.* 167 (2017) 282–289.
37. Yuvan, Y.; Choi, K.; O Choi, S.; Kim, J. Early stage release of an anticancer drug by polymer miscibility in a hydrophobic fiber-based drug delivery system. *RSC Adv.* 2018, 8, 19791–19803.
38. A. K. Singh, R. Tiwari, V. K. Singh, P. Singh, S. R. Khadim, U. Singh, V. Srivastava, S. H.
39. Manish Kumar, Samarshi Chakraborty, Pradeep Upadhaya, G. Pugazhenthil, Morphological, mechanical, and thermal features of PMMA nanocomposites containing two-dimensional Co–Al layered double hydroxide. *J. APPL. POLYM. SCI.* 2018, DOI: 10.1002/APP.45774.
40. Samarth Bhargava, Justin Jang Hann Chu, and Suresh Valiyaveetil, Controlled Dye Aggregation in Sodium Dodecylsulfate-Stabilized Poly(methylmethacrylate) Nanoparticles as Fluorescent Imaging Probes *ACS Omega* 2018, 3, 7663–7672 DOI: 10.1021/acsomega.8b00785.
41. Raza, A.; Nasir, A.; Tahir, M.; Taimur, S.; Yasin, T.; Nadeem, M. Synthesis and EMI shielding studies of polyaniline grafted conducting nanohybrid. *J. Appl. Polym. Sci.* 2021, 138, 49680.

HOW TO CITE: L. Edwin Paul, M. Shanmugavel, P. Balashanmugam, S. Thennarasu, V. Jaisankar*, Antimicrobial Characteristics Of Certain Polymeric Materials Containing Guanidine And Hydrazine Derivatives, *Int. J. of Pharm. Sci.*, 2024, Vol 2, Issue 7, 2266-2285. <https://doi.org/10.5281/zenodo.13140816>

